Mon. Not. R. Astron. Soc. **000**, 000–000 (1994) Printed 1 February 2008 (MN plain TEX macros v1.6)

Spectroscopy and orbital periods of four cataclysmic variable stars

John R. Thorstensen and Cynthia J. Taylor
Department of Physics and Astronomy, Dartmouth College, Hanover, New Hampshire, 03755 USA

ABSTRACT

We present spectroscopy and orbital periods $P_{\rm orb}$ of four relatively little-studied cataclysmic variable stars. The stars and their periods are: AF Cam, $P_{\rm orb} = 0.324(1)$ d (the daily cycle count is slightly ambiguous); V2069 Cyg (= RX J2123.7+4217), 0.311683(2) d; PG 0935+075, 0.1868(3) d; and KUV 03580+0614, 0.1495(6) d. V2069 Cyg and KUV 03580+0614 both show HeII λ4686 emission comparable in strength to Hβ. V2069 Cyg appears to be a luminous novalike variable, and the strong HeII suggests it may be an intermediate polar. The period of KUV 03580+0614 is similar to members of the SW Sex-type novalike variables, and it shows the phase-dependent absorption in the Balmer and He I lines typical of this subclass. AF Cam shows absorption features from a K-type secondary, as expected given its rather long orbital period. The secondary spectrum and the outburst magnitude both suggest that AF Cam is about 1 kpc distant. The spectrum of PG 0935+075 resembles that of a dwarf nova at minimum light, with a noticeable contribution from an M-dwarf secondary star. The secondary spectrum and a tentative outburst magnitude both suggest a distance near 500 pc.

Key words: stars: novae – stars: cataclysmic variables – binaries: close – stars: individual – stars: variables – stars: fundamental parameters

1 INTRODUCTION

Cataclysmic variable stars (CVs) are close binary systems in which a red dwarf transfers matter onto a white dwarf, generally by overflowing its Roche critical lobe. Warner (1995) gives an excellent comprehensive review of CVs.

The orbital period of a cataclysmic is a fundamental observable which correlates with evolutionary state and outburst type. In addition, the Ritter & Kolb (1998) catalog, which is heavily used by the CV community, includes only those systems with known or suspected binary periods, with the result that a system remains largely 'beneath the radar' until a period is measured. Photometry yields incontrovertible orbital periods when eclipses are present, but other modulations can masquerade as orbital periods. Radial-velocity spectroscopy is therefore the most reliable technique for determining orbital periods of non-eclipsing CVs. The long cumulative exposures needed to find reliable periods are useful for characterizing the stars in other ways as well.

We present here spectra and radial velocity periods for four CVs. Section 2 details the techniques common to the studies, Section 3 gives background information and results for the individual stars, and Section 4 contains a brief discussion.

2 TECHNIQUES

All the observations (summarized in Table 1) are from the MDM Observatory on Kitt Peak, Arizona. The 1998 January observations of KUV 03580+0614 are from the 1.3 m McGraw-Hill telescope and Mark III spectrograph, and all others are from the 2.4 m Hiltner telescope and modular spectrograph. We observed comparison lamps frequently, and checks of the λ5577 night-sky line show that our wavelength scale is typically stable to < 10 km s^{-1}. When the weather appeared photometric, we observed flux standards in twilight. Even so, our absolute fluxes are not expected to be accurate to much better than 30 per cent, because of occasional clouds and variable losses at the spectrograph slits (1 arcsec at the 2.4 m., 2.2 arcsec at the 1.3 m). Furthermore, for unknown reasons the modular spectrograph produces wavelike distortions in the continua; these appear to average out in sums of many exposures. Table 2 contains measurements of the average fluxed spectra.

The data were reduced to counts vs. wavelength at the observatory, using standard procedures within IRAF. Radial velocities of emission lines were measured using convolution algorithms described by Schneider & Young (1980) and Shafter (1983). For absorption velocities, we used the cross-correlation algorithms of Tonry & Davis (1979), as implemented in the *rvsao* package (Kurtz & Mink 1998). To search for periods we used the 'residual-gram' method described by Thorstensen et al. (1996), and to test alias choices in doubtful cases we used the Monte Carlo method explained by Thorstensen & Freed (1985). With the rough period established, we fit the velocities with sinusoids, the parameters of which are in Table 3.

We note one simple innovation in these otherwise standard procedures. As part of the spectral reduction process,

Table 1. Observing Log

Run	Nights	N	exposure (s)	Range (Å)	$\Delta\lambda$ (Å)
V2069 Cyg					
1997 Sep	3	23	360	4000 – 7500	3.7
1997 Dec	3	12	480	4000 – 7500	3.7
1998 Sep	1	3	480	4040 – 7500	3.7
1999 Jun	3	9	300	4230 – 7580	3.6
1999 Oct	4	7	240	4230 – 7550	3.9
AF Cam					
2000 Jan	5	32	360	4210 – 7560	3.6
PG 0935+075					
1996 Apr	3	27	480	4208 – 6780	2.7
2000 Jan	4	21	480	4210 – 7560	3.6
KUV 03580+0614					
1997 Dec	3	41	480	4000 – 7500	3.7
1998 Jan	4	7	900	4845 – 6865	4.5
1999 Oct	4	57	480	4230 – 7560	3.6

Exposure times listed are typical values for each run. $\Delta\lambda$ is the FWHM resolution determined from fits to night-sky features.

IRAF can estimate the noise in each spectral bin from the readout noise, detector gain, background, and so on. We have modified the convolution algorithm to compute a counting-statistics uncertainty in the radial velocities by propagating these noise estimates through the calculation. These *a priori* estimates allow the data to be more optimally weighted in period finding and curve fitting.

3 THE INDIVIDUAL STARS

3.1 AF Camelopardalis

This object is listed in the General Catalog of Variable stars (Kholopov et al. 1988) as a U Gem-type dwarf nova with $13.4 \leq m_{\rm pg} \leq 17.6$. It is the only star here with a useful period estimate in the literature. Early indications of a very short period (Szkody & Mateo 1986, Howell and Szkody 1988) prompted an emission-line radial velocity study by Szkody and Howell (1989). They obtained very limited data which indicated a 5–6 h period, leading Ritter & Kolb (1998) to tabulate $P_{\rm orb} = 0.23$: in their catalogue.

We observed this object in 2000 January, in quiescence. The mean spectrum (Fig. 1) shows the absorption features of a late-type secondary star, as would be expected given the relatively long $P_{\rm orb}$. The emission lines are conspicuous and fairly narrow. We quantified the secondary star's contribution by taking K-type main-sequence spectra from the library of Pickles (1998), scaling them by logarithmically-spaced factors, and subtracting them from the mean fluxed AF Cam spectrum, which had been smoothed to match the lower resolution of Pickles' spectra. The resulting spectra were plotted and examined by eye to find the best cancellation of the secondary star features. We found acceptable subtractions for stars of type K4, K5, and K7, and a marginal match was possible for M0. The secondary contribution was 30–40 per cent of the light near λ6500. For the secondary alone we find $V = 18.4$, with an uncertainty estimated from the decomposition and the flux calibration of perhaps ± 0.5 mag.

Table 2. Spectral Features.

Wavelength (Å)	Identification	E.W. (Å)	Flux	FWHM (Å)
AF Cam (2000 January)				
4339	Hγ	33	107:	18:
4473	HeI λ4471	9:	28:	16:
4860	Hβ	33	125	15
5876	HeI λ5876	7:	37:	15:
5893	NaD	−1.8 :	...	10:
6564	Hα	37	220	16
6680	HeI λ6678	4	23	19
7066	HeI λ7067	3:	20	24:
V2069 Cyg (1997 December)				
4340	Hγ	10	120	13
4641	CIII/NIII	3:	35:	26
4684	HeII λ4686	15	180	13
4922	HeI λ4921	2:	26	16:
5014	HeI λ5015	2:	25	12:
5411	HeII λ5411	2.5:	30	20:
5780	DIB	-0.4	...	4
5874	HeI λ5876	49	13	
5889	Na DI	-0.5	...	3.2
5895	Na DII	-0.9	...	6.3
6562	Hα	32	365	15
6678	HeI λ6678	3.8	42	16
7064	HeI λ7067	2.7	31	15
PG 0935+075 (2000 January)				
4340	Hγ	93	129	18:
4861	Hβ	80	138	18
4921	HeI λ4921	14	20:	
5018	HeI λ5015	16:	25	28:
5168	FeI λ5169	9:	16:	18:
5875	HeI λ5876	23	40:	23
6562	Hα	101	199	20:
6676	HeI λ6678	10	18	25
KUV 03580+0614 (1999 October)				
4338	Hγ	6	158	21
4647	CIII/NIII	3	67	29
4684	HeII λ4686	10	220	20
4859	Hβ	8.6	185	19
5011	HeI λ5015	0.6:	13	...
5407	HeII λ5411	0.8	14	20
5780	DIB	-0.4	...	5.8
5872	HeI λ5876	1.3:	22	22:
5890	Na D1	0.4:	...	3.4
5896	Na D2	0.4	...	4.1
6562	Hα	23	303	25
6678	HeI λ6678	2	27	25
7063	HeI λ7067	1.3:	15	24:

Wavelengths are as observed. Positive equivalent widths denote emission. Line fluxes are given in units of 10^{-16} erg cm^{-2} s^{-1}, and their estimated accuracy is $\pm$30 per cent. The secondary absorption features in AF Cam are not tabulated, with the exception of Na D. The HeI lines in PG0935+075 were strongly affected by their central absorption, and the Na D1 and HeI λ5876 lines generally overlapped.

We cross-correlated the $\lambda\lambda 5020 - 5860$ and $\lambda\lambda 5900 - 6500$ regions against a composite of several G- and K-type IAU radial velocity standards, and obtained velocities for 30 of our 32 target spectra, with typical estimated errors $\sim$ 20 km s^{-1}. We measured the Hα emission line by convolving with the derivative of Gaussian, optimized for a 16 Å

Table 3. Fits to the Radial Velocities

Data	T_0 (HJD)	P (d)	K (km s−1)	γ (km s−1)	σ (km s−1)	N
AF Cam (absn)	2451552.671(4)	0.3242(12)	104(5)	20(4)	21	30
AF Cam (emn)	2451552.497(4)	0.3230(12)	58(3)	15(3)	12	32
AF Cam (avg)	...	0.3236(9)	...	...	...	
V2069 Cyg	2451066.783(2)	0.311683(2)	125(5)	12(3)	20	53
PG 0935+075	2451552.774(2)	0.1868(3)	86(7)	−20(5)	22	42
KUV 03580+0614	2451470.668(3)	0.1495(6)	67(8)	−53(6)	42	105

Fits are of the form $v(t) = \gamma + K \sin[2\pi(t - T_0)/P]$, and σ is the uncertainty of a typical measurement judged from the scatter around the best fit. N is the number of velocities used.

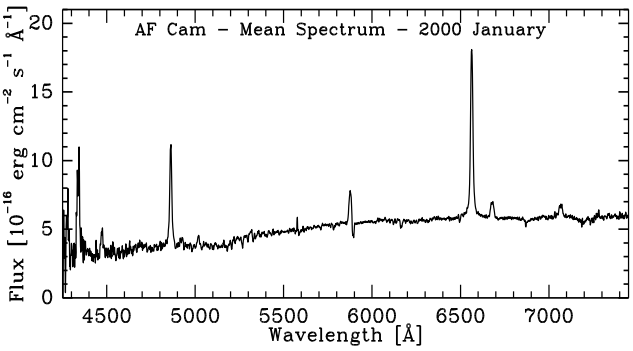

Fig. 1. Mean flux-calibrated spectrum of AF Cam, from 2000 January. The vertical scale is uncertain by perhaps 30 per cent.

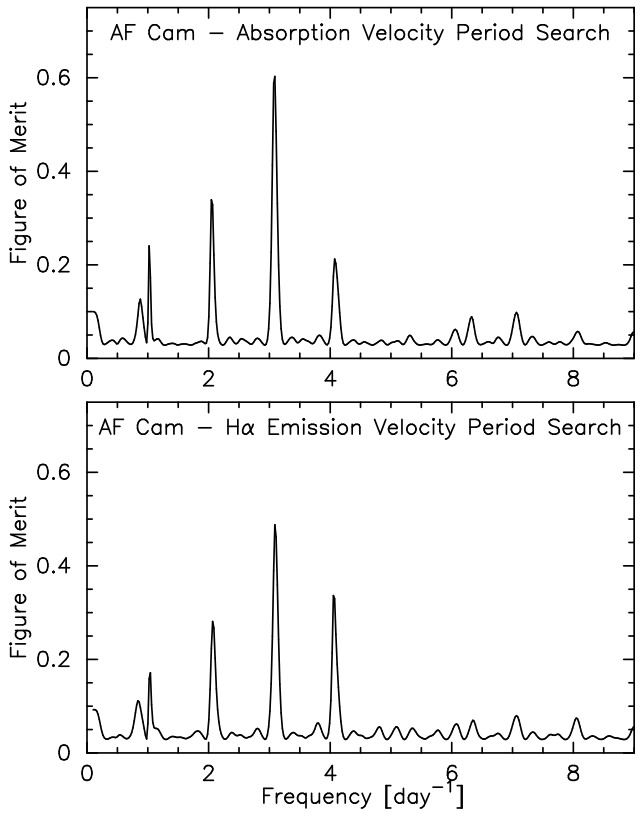

Fig. 2. Period searches of the absorption (top) and emission (bottom) velocities of AF Cam. The figure of merit shown is the inverse of $(1/N)\sum_i (o-c)^2/\sigma_i^2$, where o is the observed value, c is the value computed from the best-fit sinusoid at the trial frequency, and σ_i is the estimated uncertainty of that particular velocity.

FWHM. The counting-statistics velocity uncertainties here were typically 10 km s^{-1}. Fig. 2 shows periodograms for the emission and absorption velocities, both of which favor a period near 0.32 d, but with the inevitable daily cycle-count aliases. The Monte Carlo tests give discriminatory powers (defined in Thorstensen & Freed 1985) of 0.96 and 0.83 for the emission and absorption time series respectively, with correctness likelihoods somewhat higher than this, so the cycle count is reasonably secure, but frequencies differing by 1 cycle d^{-1} cannot be excluded absolutely. The data span 7.8 h of hour angle, ordinarily enough to decide daily cycle counts unambiguously, but the sampling is somewhat sparse and the period is awkwardly close to an integer submultiple of one day. On the face of it, Szkody & Howell's (1989) 5–6 hr period favors the ~ 4 cycle d^{-1} alias, rather than the ~ 3 cycle d^{-1} we adopt; however, their data do not have enough hour angle span to influence the choice.

Fig. 3 shows the velocities folded on the combined best period. The sine fits (Table 3) show that the emission line velocity modulation lags the absorption line velocities by 0.54 ± 0.02 cycles, suggesting as usual that the emission lines do not trace the white dwarf motion with any precision.

The secondary velocity amplitude suggests a fairly low orbital inclination, as might be expected from the single-peaked emission lines. As a purely illustrative example, the observed 104 km s^{-1} velocity amplitude of the secondary would be expected for a 0.6 $M_\odot$ secondary orbiting a 0.7 $M_\odot$ white dwarf with an inclination of 35 degrees. If the late-type features arise preferentially on the hemisphere facing away from the white dwarf, the true K is even smaller, and the inclination still lower.

The spectral type found here (K4–M0) is similar to that of other relatively long-period CVs (Beuermann et al. 1998). AF Cam appears very similar to the apparently brighter system CH UMa. The orbital period of CH UMa is 0.343 d (Friend et al. 1990), only a few per cent longer than AF Cam. Becker et al. (1982) estimate the spectral type of CH UMa's secondary as K4–M0, identical to our estimate for AF Cam.

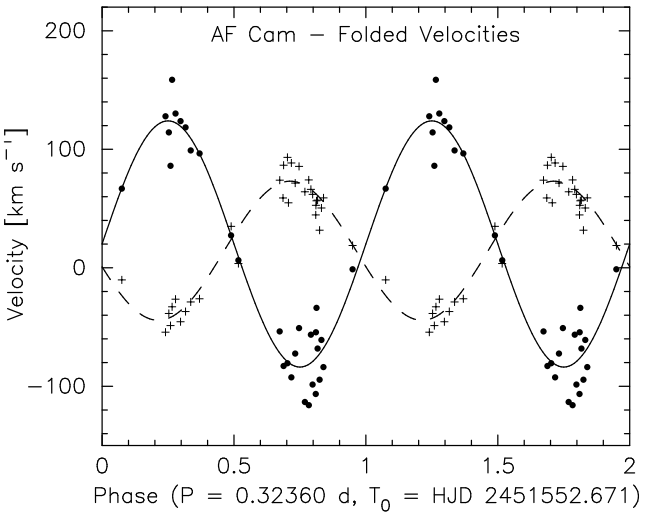

Fig. 3. Velocities of AF Cam folded on the best period. All data are plotted twice for continuity. The round dots show the absorption velocities, and the crosses the Hα emission velocities. The best-fit sinusoids are overplotted.

The detection of the secondary and the orbital period constrain the distance. Beuermann et al. (1999) tabulate absolute magnitudes, colors, and estimated radii of a sample of nearby K and M dwarfs (their Table 3). Scaling these data, we find that hypothetical 1 $R_\odot$ stars of type K4 and type M0 should respectively have $M_V = +6$ and $+7.2$. The orbital period and Roche constraints (Beuermann et al. 1998, eqn. 1) yield $(R_2/R_\odot) = f(q)0.92(M_2/M_\odot)^{(1/3)}$ at AF Cam's period, where the subscript 2 refers to the secondary star, and the function $f(q)$ is within 3 percent of unity for $q = M_2/M_1 \leq 1$. Because the secondary is likely to be modified by mass transfer (see, e. g., Beuermann et al. 1998), we do not assume a main-sequence mass-radius relation, but rather use the range of evolutionary models calculated by Baraffe & Kolb (2000) as a guide; this may not cover all possibilities, but it is arguably better than guessing. At $P_{\rm orb} = 8$ h their models span $0.36 \leq M_2/M_\odot \leq 0.99$, but the more massive secondaries are calculated to have spectral types distinctly earlier than observed here; more realistically, $M_2 \leq 0.7$ M$_\odot$. Secondaries ranging from 0.36 to 0.7 M$_\odot$ yield $0.65 < R_2/R_\odot < 0.82$, corresponding to stars 0.7 ± 0.3 magnitude fainter than otherwise identical stars with $R = R_\odot$. Combining these calculations and propagating the uncertainties in quadrature yields $M_V = 7.3 \pm 0.7$ for the secondary. Our detection of the secondary therefore yields yields $m - M = 11.1 \pm 0.9$.

Warner (1987, 1995) gives a relation for dwarf novae between M_V at maximum light, orbital inclination, and orbital period. The inclination is uncertain, but likely to be fairly low as noted earlier. Taking $i = 30$ degrees, these relations give $M_V(\max) = 3.0$ for AF Cam. For the apparent magnitude we use the GCVS outburst magnitude $m_pg = 13.4$, which should be similar to V for typical outburst colors. This then yields $m - M = 10.4$, in reasonable agreement with the distance estimated from the secondary. The actual distance is likely to be less, because of extinction corrections at this low Galactic latitude ($b = 2^\circ.2$).

3.2 V2069 Cygni

V2069 Cyg (= RX J2123.7+4217) was discovered through its X-ray emission by Motch et al. (1996). They presented a spectrum and a 2.8-hour session of time-resolved CCD photometry, which showed flickering but no apparent periodicity. It is listed as 'Cyg6' in Downes, Webbink, and Shara's (1997) catalog and atlas of CVs (hereafter DWS97).

The spectrum (Fig. 4) appears similar to that in Motch et al. (1996). The He II λ 4686 line is notably strong. The equivalent width of NaD (which does not show orbital motion) and the continuum slope both suggest that the reddening is not negligible. The Hα radial velocities were measured using the derivative of a gaussian as the convolution function, optimized for 14 Å FWHM. The period search (Fig. 5) yielded a unique choice of cycle count for the 760-day span of the observations. The resulting period, 0.311683(2) d, or 7.48 h, is determined with the greatest accuracy of those reported here. The folded velocities (Fig. 6) and fits (Table 3) show why this went so well – the velocity amplitude K was was large, and the scatter relatively small, making the periodic modulation very conspicuous.

V2069 Cyg shows several features in common with V405 Aur (= RX J0558+5353). They are: (1) relatively narrow, single-peaked lines; (2) strong HeII λ4686 emission; (2) $P_{\rm orb} > 4$ h; (3) a quiet, large-amplitude emission-line radial velocity curve. V405 Aur has proven to be a very interesting DQ Her star (= intermediate polar; see Harlaftis & Horne 1999 and references therein). Although Motch et al.'s (1996) brief light curve did not show obvious periodic pulsation, a more sensitive search might be rewarded with success.

3.3 PG 0935+075

PG 0935+075 was discovered as an ultraviolet-excess object in the Palomar-Green survey (Green, Schmidt, & Liebert 1986). Ringwald (1993) obtained a spectrum showing the strong, broad Balmer and He I emission typical of a cataclysmic binary. DWS97 list the object as 'Leo7'. It is evidently a little-studied dwarf nova, since it appears at $B = 13.0$ in the PG survey, but is much fainter in Ringwald's spectrum and in the observations described below.

We observed this object only in 1996 April and 2000 January. The 1996 April observations indicated a periodicity near 0.19 d, but the daily cycle count was ambiguous. The 2000 January observations, though fewer in number, were arranged to span 7.35 h of hour angle and therefore decided the daily cycle count. The periods derived from the two observing runs differ by almost twice their mutual standard deviation, but are reasonably consistent, with a weighted average of 0.1868(3) d. Because the two observing runs were so far apart, there is no unique choice of cycle count between them, but if the two runs are phase coherent the allowed periods are expressed by $(1371.151 \pm 0.003$ d$)/(7345 \pm 50)$, where the denominator is an integer. Because of the mediocre agreement of the individual runs' periods, the cycle-count uncertainty is chosen to yield periods within $\pm 4\sigma$ of the weighted average. Fig. 7 summarizes the period search for the velocities, and Fig. 8 shows the folded velocities.

The mean spectrum (Fig. 9, Table 2) closely resembles those of dwarf novae at minimum light. There is a contribution from an M-dwarf secondary star, which confirms that the luminosity was fairly low when the data were taken.

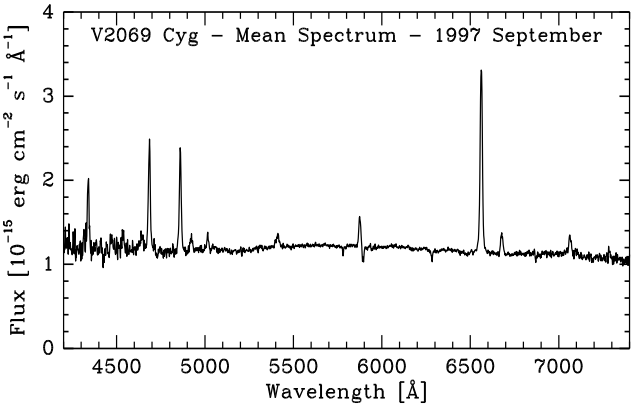

Fig. 4. Mean spectrum of V2069 Cyg. Note the relatively narrow emission lines and the strength of HeII λ4686.

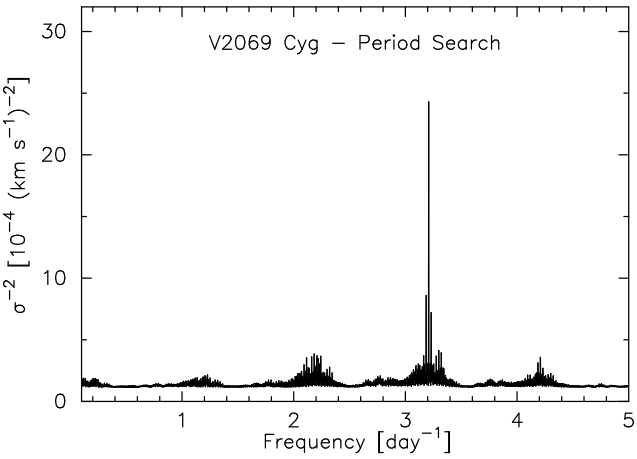

Fig. 5. Period search of the Hα emission velocities of V2069 Cyg. The vertical axis is the mean of the inverse square residual at each frequency. A single frequency is strongly preferred.

It would appear from the spectrum, period, and the minimal information available on variability that this object is a UGSS.

To quantify the secondary star contribution we used the subtraction technique described earlier, but this time with a library of M-dwarf spectra classified by Boeshaar (1976) and observed with the same instrumental setup. We found the secondary contribution to be type M3 $\pm$ 1, with the secondary contributing 45 ± 15 per cent of the continuum at 6500 Å. The secondary contribution has $V = 19.7 \pm 0.5$. Unfortunately, this was too faint for us to measure radial velocities of the secondary.

Again, we can estimate a distance from the secondary contribution. Adapting the data from Table 3 of Beuermann et al. (1999), we find that a hypothetical $1R_\odot$ star of type M3 $\pm$ 1 would have $M_V = 9.2 \pm 1.0$. The Roche lobe constraint at this period yields $R_2/R_\odot = 0.64 f(q)(M_2/M_\odot)^{(1/3)}$. Turning again to the evolutionary models of Baraffe & Kolb (2000), we find $0.17 \leq M_2/M_\odot \leq 0.6$ in the 4–5 hour period range, which gives $0.35 \leq R_2/R_\odot \leq 0.54$, ignoring the slight variation in $f(q)$. This makes the secondary 1.8 ± 0.5 mag fainter than a $1R_\odot$ star of the same spectral class, so we estimate $M_V = 11.0 \pm 1.2$ for the secondary, which in turn yields $m - M = 8.7 \pm 1.3$. The uncertainty in the secondary's spectral type dominates the error budget. For comparison, Warner's (1987) maximum light relationship yields $M_V(\mathrm{max}) = 4.6$ at this period. Taking the inclination correction as zero and V at minimum light as 13.0 (both quite uncertain) yields $m - M = 8.4$. The good agreement should probably be interpreted as supporting the dwarf nova classification of this star (that is, on the one occasion it was seen to be bright, it was about as bright as expected for a dwarf nova), rather than as corroborating the distance. At $b = +40.2$, the extinction is unlikely to be significant. If $m - M = 8.7$, PG0935+075 lies some 350 pc from the Galactic plane.

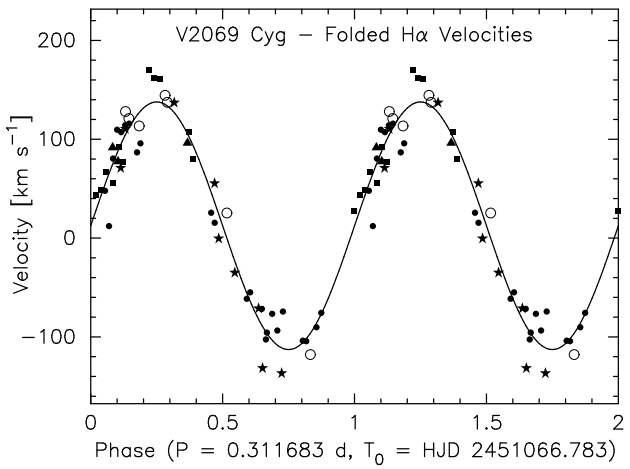

Fig. 6. Hα radial velocities of V2069 Cyg, folded on the best period. Different symbols represent different observing runs as follows: solid dots, 1997 Sept.; filled squares, 1997 Dec.; filled triangles, 1998 Sept.; stars, 1999 June; and open circles, 1999 Oct.

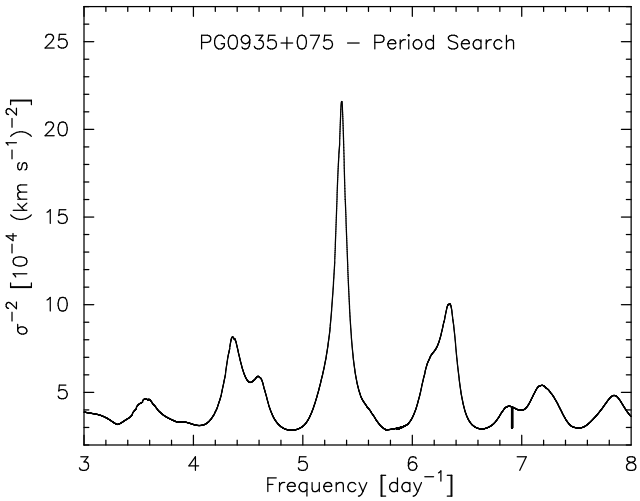

Fig. 7. Period search of Hα radial velocities of PG0935+075. The full periodogram shows ringing from the unknown number of cycle counts between the widely-spaced observing runs, so the curve shown here is formed by connecting the local maxima of the periodogram with straight lines.

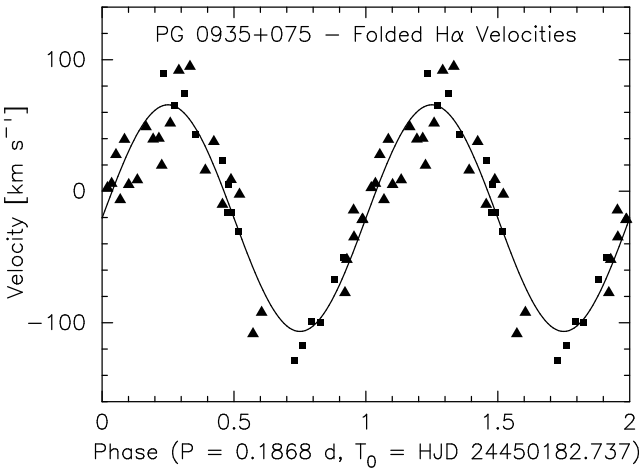

Fig. 8. Hα radial velocities of PG0935+075 folded on the best period. The period used reflects an essentially arbitrary choice of cycle count between observing runs. Filled triangles are from 1996 April, and filled squares from 2000 January.

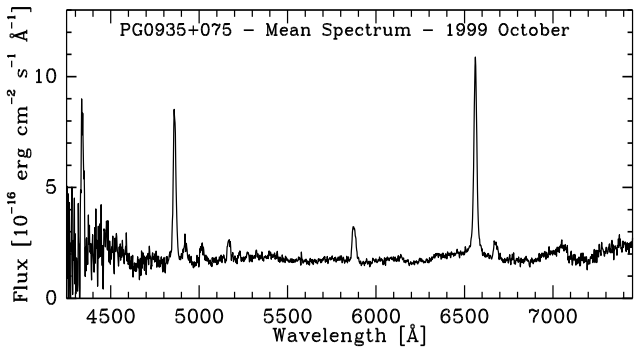

Fig. 9. Mean spectrum of PG0935+075 from 1999 October. Note the M dwarf features.

3.4 KUV 03580+0614

Wegner & Boley (1993) discovered that KUV 03580+0614 shows emission lines, and flagged it as a cataclysmic variable candidate. DWS97 list it as 'Tau2'.

The 1997 December velocities indicated a period near 0.15 d, but the daily cycle count was not securely established. The 1999 October data are slightly more extensive and the velocities show less scatter; they unambiguously confirm the 0.15 d period. Sinusoidal fits to velocities from the two observing runs starting near this frequency gave essentially the same period, the weighted average being 0.1495 ± 0.0006 d. A period search of the combined velocities yields a slightly longer best-fit period near 0.1502 d. The cycle count between the observing runs is not determined, but the periods within $\pm 3\sigma = 0.0018$ d of the best overall period can be expressed as $(671.772 \pm 0.005 \text{ d})/(4472 \pm 53)$, the denominator being integer. Figures 10 and 11 show the period search and the folded radial velocities.

Fig. 12 shows the mean spectrum from 1999 October; the 1997 spectrum appeared generally similar with a slightly

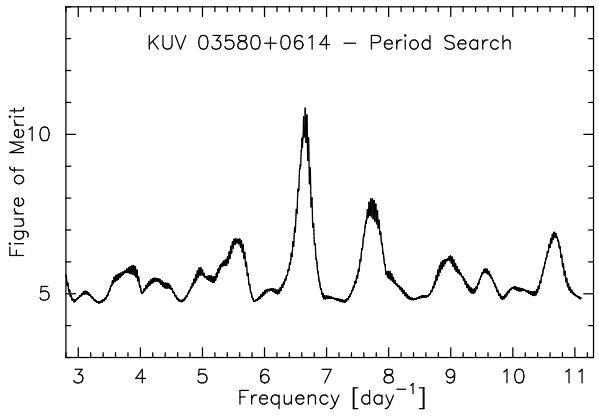

Fig. 10. Period search of Hα radial velocities of KUV 03580+0614. The curve shown here is formed by connecting the local maxima of the periodogram with straight lines.

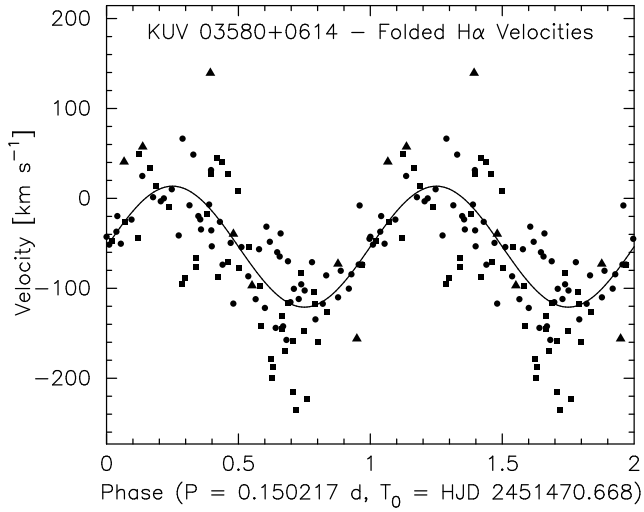

Fig. 11. Hα radial velocities of KUV 03580+0614 folded on the best period. The period used reflects an essentially arbitrary choice of cycle count between observing runs. Filled squares are from 1997 December, filled triangles from 1998 January, and solid circles are from 1999 October.

lower flux level. The spectrum is that of a novalike variable, with HeII λ4686 similar in strength to Hβ; the continuum is quite blue, approximately $F_\lambda \propto \lambda^{-1.7}$. Fig. 13 shows a single-trailed representation of the 1999 October data, prepared using phase-averaging techniques (Taylor, Thorstensen, & Patterson 1999) The He I features especially show the distinctive phase-dependent absorption characteristic of the SW Sex stars (Thorstensen et al. 1991, Taylor et al. 1999, Dhillon, Marsh, & Jones 1998). In the SW Sex stars the Balmer emission velocities typically lag the expected white-dwarf motion by ~ 0.2 cycle. Assuming this to be the case here, we infer that white dwarf superior conjunction should occur near $\phi = 0.3$ in the phase convention we are using. In most SW Sex stars the phase of white dwarf superior conjunction is marked by eclipses, and the absorption reaches maximum strength approximately opposite the eclipse, at 'phase 0.5' in the eclipse ephemeris. This should correspond to $\phi \sim 0.8$ in the present phase convention. The

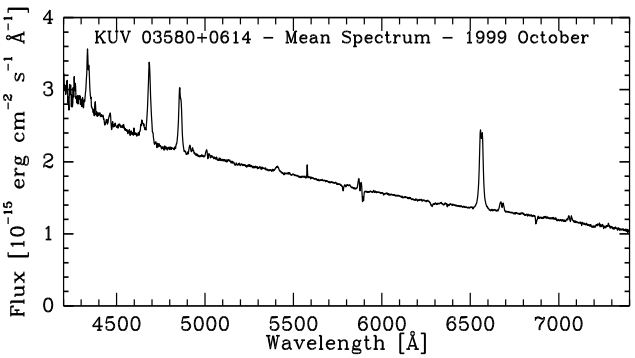

Fig. 12. Mean spectrum of KUV 03580+0614 from 1999 October. Note the strong continuum and HeII λ4686 emission.

observed absorption is strongest around $\phi \sim 0.73$, in fair agreement with expectation. Close examination of Fig. 13 also shows a red-to-blue drift of the absorption features as they strengthen, a behaviour seen in other SW Sex stars. The orbital period is also similar to other examples of the class.

A search for eclipses by R. Fried and J. Patterson (private communication, 2000) proved negative. Thus KUV 03580+0614 joins the ranks of stars which behave spectroscopically like SW Sex stars, but which do not eclipse (e.g., Taylor et al. 1999).

4 DISCUSSION

The spectra and orbital periods presented here show all these objects to be fairly typical examples of their classes.

The two dwarf novae (AF Cam and PG0935+075) are of interest largely because their secondaries are detected, which allows us to determine distances and further characterise CV secondaries. PG0935+075 should be monitored for further outbursts to confirm its variability type.

The two novalikes, V2069 Cyg and KUV 03580+0614, are potentially more interesting as individuals. V2069 Cyg shows similarities with V405 Aur, which has proven to be a very interesting DQ Her star. SW Sex stars frequently show interesting 'permanent superhumps' (which might more accurately be called persistent superhumps) in their light curves (Patterson & Skillman 1994). Thus more thorough time-series photometry of these stars may prove interesting.

KUV 03580+0614 is a good example of a star showing the phase-dependent absorption of the SW Sex phenomenon, but no eclipses. The growing number of non-eclipsing SW Sex stars presents a challenge to scenarios which require the line of sight to graze the rim of the disk (e.g., Hellier 1998). If the light being absorbed arises near the disk center, the absorbing material must be rather far from the disk plane (to be visible at non-eclipsing inclinations) and not azimuthally symmetric (to be visible only at certain phases). How this material gets there is unknown.

ACKNOWLEDGMENTS

We thank Joe Patterson and Bob Fried for communicating that KUV 03580+0614 does not eclipse, and Patrick Schmeer for a discussion of the variability of PG0935 +075. The US National Science Foundation supported this work through grants AST 9314787 and AST 9987334. The MDM Observatory staff provided cheerful and efficient help.

REFERENCES

Baraffe, I., Kolb, U. 2000, MNRAS, 318, 354
Becker, R. H., Wilson, A. S., Pravdo, S. H., Chanan, G. A. 1982, MNRAS, 201, 265
Beuermann, K., Baraffe, I., Kolb, U., Weichhold, M. 1998, A&A, 339, 518
Beuermann, K., Baraffe, I., Hauschildt, P. 1999, A&A, 348, 524
Boeshaar, P. 1976, Ph. D. Thesis, Ohio State University
Dhillon, V. S., Marsh, T. R., Jones, D. H. P. 1998, MNRAS, 291, 694
Downes, R. A., Webbink, R. F., Shara, M. M. 1997, PASP, 109, 345
Friend, M. T., Martin, J. S., Connon Smith, R., Jones, D. H. P. 1990, MNRAS, 246, 654
Green, R. F., Schmidt, M., Liebert, J. 1986, ApJS, 61, 305
Harlaftis, E. T., Horne, K. 1999, MNRAS, 305, 437
Hellier, C. 1998, PASP, 110, 420
Howell, S. B., Szkody, P. 1988, PASP, 100, 224
Kholopov, P. N. et al., 1988, General Catalogue of Variable Stars, Moscow: Nauka Publishing House.
Kurtz, M. J., Mink, D. J. 1998, PASP, 110, 934
Motch, C., Haberl, F., Guillout, P., Pakull, M., Reinsch, K., Krautter, J. 1996, A&A, 307, 459
Patterson, J., Skillman, D. R. 1994, PASP, 106, 1141
Pickles, A. J. 1998, PASP, 110, 863
Ringwald, F. A. 1993, PhD thesis, Dartmouth College
Ritter, H., Kolb, U. 1998, A&AS, 129, 83
Schneider, D. P., Young, P. 1980, ApJ, 238, 946
Shafter, A. W. 1983, ApJ, 267, 222
Szkody, P., Mateo, M. 1986, AJ, 92, 483
Szkody, P., Howell, S. B., 1989, AJ, 97, 1176
Taylor, C. J., Thorstensen, J. R., Patterson, J. 1999, PASP, 111, 184
Thorstensen, J. R., Freed, I. W. 1985, AJ, 90, 2082
Thorstensen, J. R., Patterson, J. Thomas, G., Shambrook, A. 1996, PASP, 108, 73
Tonry, J., Davis, M. 1979, AJ, 84, 1511
Warner, B. 1987, MNRAS, 227, 23
Warner, B. 1995, Cataclysmic Variable Stars (Cambridge: Cambridge U. Press)
Wegner, G., Boley, F. I. 1993, AJ, 105, 660

This paper has been produced using the Royal Astronomical Society/Blackwell Science TEX macros.

Fig. 13. (separate jpg file) Single-trailed representation of the KUV 03580+0614 spectra from 1999 October. The greyscale in the lower panel is chosen to emphasize weaker features. The upper panel shows the same data, scaled to make visible the behaviour of the stronger emission lines. The scale is negative (black = bright). In each panel, the data are ordered by phase and shown twice for continuity. The individual spectra were divided by a fitted continuum. Note the phase-dependent absorption features, especially prominent in the He I lines ($\lambda\lambda$5876, 4921, 5015, and 6678).


This figure "thorfig13.jpg" is available in "jpg" format from:
http://arXiv.org/ps/astro-ph/0105499v1